Unfolding of Nucleosomes by Ethidium Binding†

Hen-Ming Wu, Nanibhushan Dattagupta, Michael Hogan, and Donald M. Crothers*

ABSTRACT: We report spectroscopic, hydrodynamic, and biochemical studies on the complex of ethidium bromide with 140 base pair nucleosomal core particles. Fluorescence titration indicates a greater intrinsic affinity of ethidium for nucleosomes than for DNA, and fluorescence depolarization measurements imply increased immobilization of ethidium bound to nucleosomes, but with more extensive dye–dye energy transfer compared to DNA-bound dye. Ethidium intercalated into DNA in nucleosomes has a limiting reduced linear dichroism of −0.45 at 320 nm and −0.25 at 530 nm. Both the energy transfer and dichroism results are consistent with clustering of the nucleosome-bound dye molecules. Electric dichroism measurements and ultracentrifugation studies reveal that structural distortion of the nucleosome accompanies ethidium binding, occurring in the range of r (ethidium residues per base pair) values from 0.02 to 0.06. The distortion transition is characterized by an increase in the negative limiting reduced dichroism from 0.29 to 0.45 at 265 nm, an increase in the field-induced viscosity-limited rotational orientation time from 0.8 to 3 μs, and a decrease in sedimentation coefficient from 10.5 to 8.2 S. The complex was modeled hydrodynamically as a cylinder of 335-Å length and 67-Å diameter, containing 1.4 superhelical turns of DNA. Dimethylsuberimidate cross-linked nucleosomes, or native nucleosomes in the presence of Mg^{2+}, bind ethidium weakly and are not distorted. The periodicity of cutting sites produced by DNase II digestion of nucleosomes remains constant as ethidium is added, but the bandwidth increases. A thermodynamic model is proposed to interpret the binding isotherm, based on enhancement of drug binding affinity due to release of superhelical stress in the nucleosome–ethidium complex.

Recent evidence suggests that transcriptionally active genes and replicating chromatin contain bound histones but that the chromatin conformation in such regions may be partially unfolded or otherwise altered from its state in inactive chromatin (Richards et al., 1977; Lacy & Axel, 1975; Gottesfeld et al., 1975; Foe et al., 1976; Seale, 1978; Weintraub & Groudine, 1976; Garel & Axel, 1976). One can imagine both enzymatic and physical mechanisms by which the conformations of nucleosomes or other chromatin subunits could be changed. A simple example of a physical interaction is provided by the intercalating drug ethidium which binds strongly to naked DNA, unwinding the duplex by about 26° (Wang, 1974). Such a distortion of DNA could easily lead to conformational alteration of chromatin subunits.

Ethidium has been used previously as a probe for studying the structure of DNA in chromatin and nucleosomes, with a variety of spectroscopic techniques utilized for characterization of the complex (Angerer et al., 1974; Angerer & Moudrianakis, 1972; Lapeyre & Bekhor, 1974; Lawrence et al., 1976; Paoletti et al., 1977). Based on analysis of binding isotherms and fluorescence depolarization, it has been inferred that the linker or spacer region between nucleosomes contributes to the apparent small number of strong binding sites.

Our studies reported here focus on ethidium binding to isolated 140 base pair nucleosomes and the structural distortion induced by drug binding. We have utilized fluorescence titration and polarization measurements to characterize the binding equilibrium, while nucleosomal conformational changes were examined by the technique of transient electric dichroism. The results indicate that nucleosomes have a very high affinity for the first ethidium molecules bound (roughly 10 per nucleosome) in 13 mM ionic strength and that ethidium binding strongly distorts the conformation of the nucleosome. We propose a specific model for the structure of the ethidium–nucleosome complex.

Materials and Methods

The 140 base pair nucleosome core particles and DMS[1]-cross-linked nucleosomes were prepared as previously described (Wu et al., 1979). Ethidium bromide was purchased from Sigma Chemical Co. and was crystallized from 1-butanol before use.

The equilibrium binding isotherm for interaction of ethidium bromide with nucleosomes was measured by fluorescence enhancement of the dye due to complex formation. The excitation and emission wavelengths were 520 and 600 nm, respectively. The isotherm was calculated as described by Lepecq & Paoletti (1967).

Polarization of fluorescence was measured on a device kindly made available by L. Stryer, Stanford University. The excitation and emission monochromators were set at 520 and 600 nm, respectively. The four components of the polarized emitted light I_{vv}, I_{vh}, I_{hv}, and I_{hh} were measured and used to calculate the polarization ratio P by using the relationship

$$P = \frac{I_{vv} - I_{vh}t}{I_{vv} + I_{vh}t}$$

where

$$t = I_{hv}/I_{hh}$$

is a constant for the machine and was found to be 1.08 ± 0.01. The ethidium concentration was varied by direct addition of aliquots of a concentrated solution of the dye in TE buffer (10 mM Tris and 1 mM EDTA; pH 7.5 at room temperature). The contribution of free ethidium was neglected in the calculation of P.

Electric dichroism was measured on a device described elsewhere (Hogan et al., 1978; Crothers et al., 1978). The

† From the Department of Chemistry, Yale University, New Haven, Connecticut 06520. *Received August 15, 1979.* Supported by a grant, CA 15583, from the National Cancer Institute.

[1] Abbreviations used: DMS, dimethylsuberimidate; MBA, *N,N'*-methylenebis(acrylamide); EB, ethidium bromide; NC, nucleosomes; TE, buffer containing 10 mM Tris-HCl and 1 mM Na_2EDTA, pH 7.5.

0006-2960/80/0419-0626$01.00/0

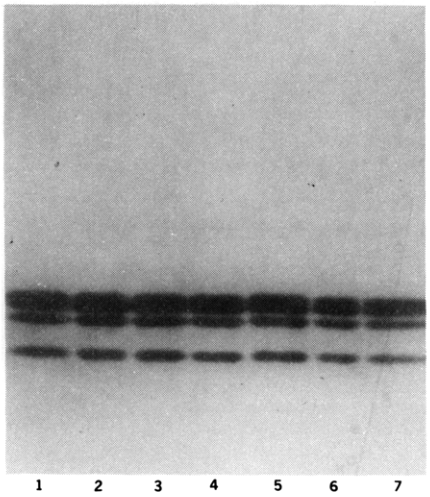

FIGURE 1: NaDodSO$_4$–15% polyacrylamide gel electrophoresis of histones present in nucleosomes isolated from isokinetic sucrose gradients (C_t = 5%; C_r = 27%) in the presence of free ethidium and TE buffer. The amount of free ethidium required to give the designated r values (EB per base pair) was calculated from the binding isotherm (see below). From left to right: (1) r = 0 (EB – free control); (2) r = 0.01; (3) r = 0.02; (4) r = 0.04; (5) r = 0.06; (6) r = 0.1, from the faster sedimenting edge of the peak; (7) r = 0.1, from the slower sedimenting edge of the peak.

reduced dichroism ρ can be calculated from the parallel component of the absorption

$$\rho = 1.5\frac{\Delta A_{\parallel}}{A}$$

where $\Delta A_{\parallel}$ is the field-induced change in absorption of a sample when the incident light is polarized parallel to the field axis. Moreover, it has been shown (Rill, 1972; Crothers et al., 1978) that for a superhelix orienting with the superhelix axis parallel to the field, the dichroism ρ_∞ at maximum orientation is related to the pitch angle (β) and transition moment angle (α) by the relationship

$$\rho_\infty = \frac{3}{4}(3\cos^2\alpha - 1)(3\cos^2\beta - 1) \qquad (1)$$

in which β is measured relative to the superhelix axis and α is measured relative to the double-helix axis.

Sedimentation coefficients were determined on a Spinco Model E analytical ultracentrifuge.

Nuclease Digestion of Nucleosomal Core Particles. Aliquots of 20 μg of native or DMS-cross-linked nucleosomal core particles were digested by 2 units of DNase II (Worthington) in 10 mM Tris-HCl, 1 mM EDTA (pH 7), and EB concentrations ranging from r = 0 to r = 0.1, with a final reaction volume of each sample of about 50 μL. All digestions were performed in the dark at 20 °C for 30 min. The digestion was stopped by quenching on ice and incubating at 100 °C for 3 min, after which samples were incubated with 10 μg of proteinase K (Merck) at 37 °C for 60 min. Subsequently, 30 μL of 10 M urea and 10 μL of tracking dye solution were added to each sample and incubated for 1 min at 100 °C. The aliquots were directly applied to a 7 M urea–8% polyacrylamide gel with 1.25% MBA as described by Lutter (1979). DNase I digestions were performed as described for DNase II digestions above, except that the solvent was 10 mM Tris-HCl and 10 mM Mg^{2+} (pH 7) and the reaction was stopped by adding 5 μL of 250 mM EDTA and quenching on ice. Gels were stained with ethidium and photographed with UV transillumination and a red filter.

Analytical Procedure. To assay the association of histones with DNA in nucleosome–EB complexes, we ran the particles through an isokinetic gradient (C_t = 5%; C_r = 27%) containing the appropriate free EB concentration (calculated from the equilibrium binding isotherm) in an SW40 rotor at 38 krpm for 24 h. The nucleosome–EB peaks were collected, lyophilized, and loaded onto 15% NaDodSO$_4$–polyacrylamide histone gels.

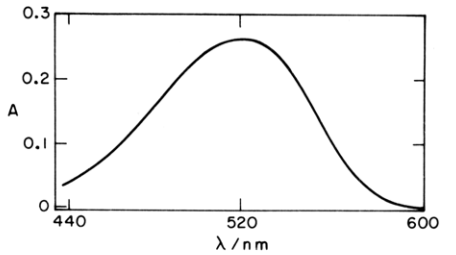

FIGURE 2: Absorption spectrum of a nucleosome–ethidium complex. TE buffer; r_{added} = 0.075; nucleosome concentration was 8.53 × 10^{-4} M DNA base pairs; T = 20 °C.

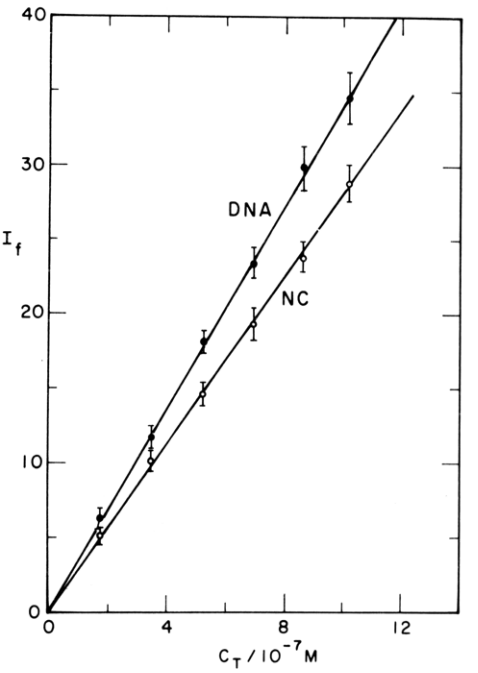

FIGURE 3: Fluorescence enhancement of EB due to complex formation in TE buffer at 20 °C. Excitation wavelength = 520 nm; I_f = total fluorescence intensity (arbitrary units); C_T = total added ethidium concentration. Nucleosome (NC) concentration = 2.3 × 10^{-5} M DNA base pairs; DNA concentration = 2.7 × 10^{-5} M base pairs.

Results

Core histones remain associated with the ethidium–nucleosome complex. Figure 1 shows the results of NaDodSO$_4$–polyacrylamide gel electrophoresis analysis of the histones present in EB–nucleosome complexes isolated from ethidium-containing isokinetic sucrose gradients. We detected no change in the relative amounts of core histones present, even up to bound ethidium amounts of r = 0.1 (EB per DNA base pair). Hence, we conclude that the nucleosome–ethidium complex is stable and a suitable object for physical studies.

The absorbance properties of ethidium bound to nucleosomes and to free DNA are identical. Figure 2 shows the absorbance spectrum of EB bound to nucleosomes in TE buffer at r = 0.075 (ethidium residue per base pair). The spectrum displays a maximum at 520 nm, with an extinction coefficient of 4200 ± 200 M^{-1} cm^{-1}. These parameters are identical within experimental accuracy with those observed for EB intercalated into free DNA (Bresloff & Crothers, 1975).

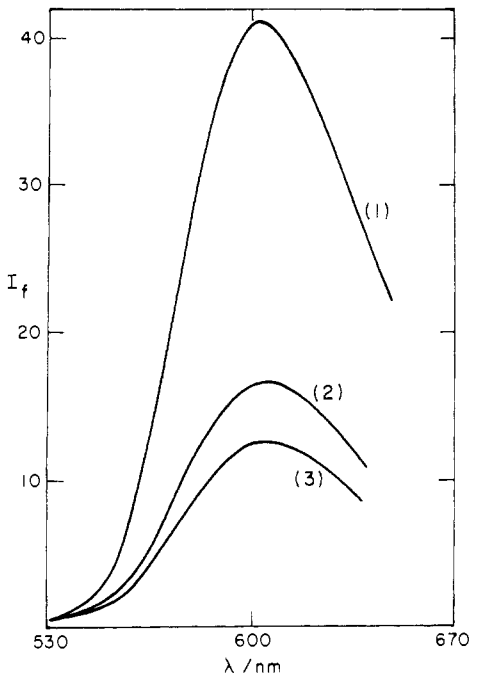

FIGURE 4: Corrected fluorescence emission spectrum of the EB–NC complex at $r = 0.074$ and [NC] = 9.42×10^{-5} M in TE buffer at 20 °C. (1) No polarization; (2) polarizers vertical/vertical; (3) polarizers vertical/horizontal. Excitation wavelength = 520 nm.

Fluorescence measurements suggest that ethidium is intercalated into DNA in nucleosomes. Figure 3 shows the fluorescence intensity (I_f) for EB binding to 140 base pair calf thymus DNA and 140 base pair nucleosomes (NC). Linearity of I_f with ethidium concentration is consistent with quantitative binding under these concentration conditions, as also verified by subsequent titration at lower DNA and NC concentrations. The smaller slope for nucleosomes in Figure 3 indicates that the intrinsic fluorescence enhancement for bound EB is 83 ± 5% as large when the complex is formed with nucleosomes, compared to free DNA. The observed emission spectrum (Figure 4), corrected with a rhodamine standard for wavelength variation of the optical sensitivity, is identical with that observed for free DNA (Lepecq & Paoletti, 1967). The free EB concentration contributes less than 4% to the total fluorescence intensity for the conditions of the experiment in Figure 4.

An intense 606-nm fluorescence emission maximum has been shown to accompany EB intercalation into double-helical DNA. When bound to single-stranded DNA or to polyphosphates, ethidium shows a small fluorescence enhancement, only 5–10% of that of the intercalated complex (Lepecq & Paoletti, 1967). Therefore, the fluorescence properties of EB bound to nucleosomes are consistent with intercalative binding.

The affinity of ethidium is greater for nucleosomes than for free DNA when r is small. Figure 5 shows Scatchard (1949) plots of fluorescence titration data for ethidium binding to nucleosomes and to free 140 base pair DNA. The two isotherms cross at $r = 0.07$ (ethidium per base pair), for which the free ethidium concentration $m = 0.2$ μM. Hence, at ethidium concentrations below 0.2 μM ($0.04 \leq r < 0.07$), nucleosomes bind more ethidium than the same amount of free DNA, whereas the opposite is true when the ethidium concentration exceeds 0.2 μM.

Fluorescence polarization implies increased immobilization of EB bound to nucleosomes, with more extensive dye–dye energy transfer, compared to DNA-bound dye. Figure 6 compares the concentration dependence of the fluorescence

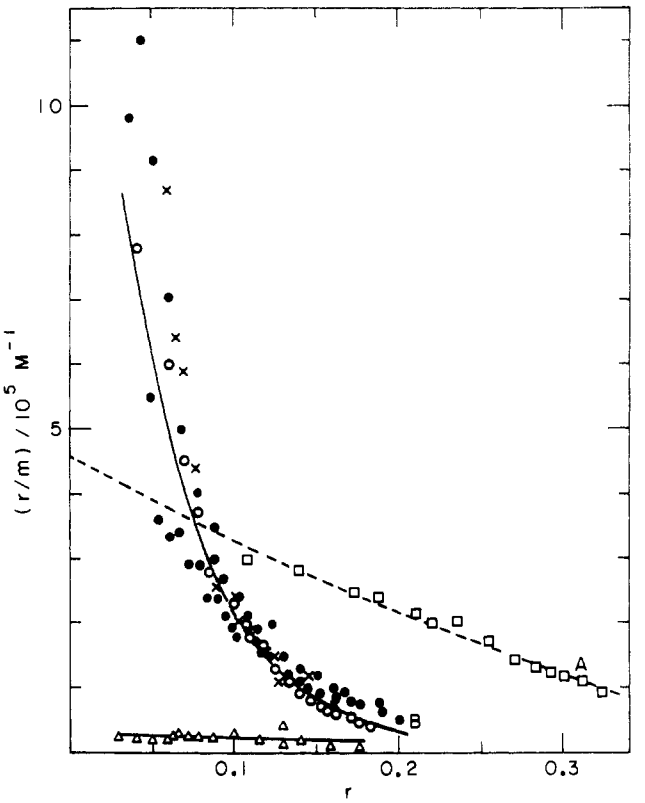

FIGURE 5: Scatchard plot of the equilibrium binding isotherm of ethidium for nucleosomes and free DNA, determined by fluorescence titration. TE buffer, 20 °C. r = EB per DNA base pair; m = free ethidium concentration. (□) Free DNA; (●, ○, and ×) 140 base pair core nucleosomes from different preparations; (△) DMS-cross-linked nucleosomes. The dashed line in (A) is the theoretical neighbor exclusion isotherm, and the solid line in (B) is the theoretical binding isotherm for the model described under Discussion.

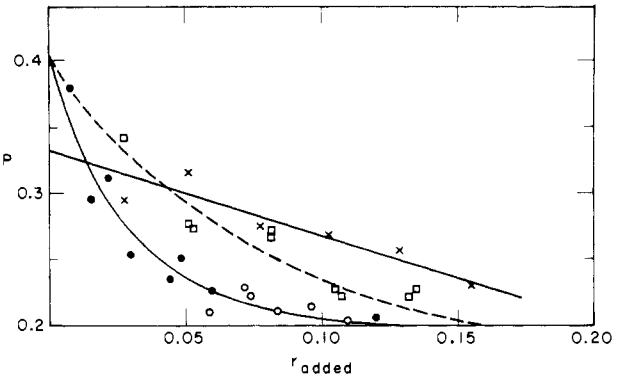

FIGURE 6: Fluorescence polarization P of EB bound to DNA and NC in TE buffer, 20 °C. r_{added} = EB added per DNA base pair. (×) DNA, 5.45×10^{-5} M base pairs; (●) NC, 9.42×10^{-5} M DNA base pairs; (○) NC, 5.8×10^{-5} M DNA base pairs; (□) NC, 5.15×10^{-5} M DNA base pairs, plus 33% sucrose.

polarization P for EB bound to nucleosomes and to 140 base pair free DNA. At low r values the degree of polarization of NC-bound EB approaches 0.4, which is the limit seen for EB intercalated into DNA or nucleosomes in high-viscosity media. In aqueous media at $r \simeq 0$ the polarization of DNA-bound EB is smaller than that of NC-bound EB. This implies greater rotational freedom of the drug when bound to free DNA. According to the analysis given by Barkley & Zimm (1979), depolarization is due both to "wobble" of the dye in its intercalation site and to bending and torsional motions of the DNA chain. Apparently all of these motions are relatively suppressed in DNA incorporated into nucleosomes. A similar

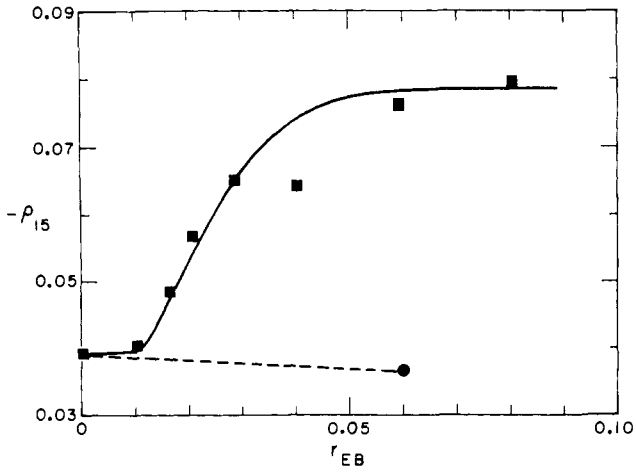

FIGURE 7: Effect of EB on the electric dichroism of nucleosomal particles. ρ_{15} is the measured reduced dichroism amplitude at 265 nm and 15 kV potential difference (12.3 kV/cm electric field). T = 4 °C; TE/3 buffer (ionic strength 4.3 mM). (■) NC; (●) DMS-cross-linked nucleosome.

conclusion was reached by Bontemps & Fredericq (1974) for ethidium bound to nucleohistone.

As r increases, the fluorescence polarization drops more rapidly for EB bound to NC than to DNA (Figure 6), even in a viscous medium. This result probably reflects EB–EB energy transfer, for which the characteristic Förster distance R_0 is 15–16 Å (Paoletti & Lepecq, 1971). Clustering of bound dyes in the NC–EB complex would account for more extensive energy transfer in this case. It is also possible that energy transfer occurs between dyes bound to successive turns of the nucleosome superhelix, although the expected center-to-center distance (≥25 Å) between donor and acceptor exceeds R_0 substantially.

The amplitude of the reduced electric dichroism indicates that the nucleosome is structurally altered due to ethidium binding. Figure 7 shows the variation of the reduced electric dichroism amplitude at 265 nm with increasing amount of ethidium bromide. The change of $-\rho$ at 15 kV is sigmoidal with r, and at about r = 0.06 the amplitude reaches a plateau value. The variation of dichroism with field strength at 320 and 265 nm is shown in Figure 8. It can be seen from the figure that the average orientation of the 320-nm transition moment and the overall orientation of the DNA base transition moments relative to the field must be the same.

Since the dichroism at any wavelength is the weighted sum of all the contributing transition moments, the dichroism at 265 nm for the EB–NC complex is given by

$$\langle\rho\rangle_{obsd} = \frac{\rho_{DNA}A_{DNA} + \rho_{EB}A_{EB}}{A_{DNA} + A_{EB}} \approx \rho_{DNA}$$

where the latter equality results because the ethidium dichroism contribution ρ_{EB} at 265 nm is expected to be approximately the same as that at 320 nm [both the 320- and 280-nm transitions of EB are thought to be polarized along the long molecular axis (Houssier et al., 1974; Hudson & Jacobs, 1975)]. At 530 nm, where the transition moment is directed along the short axis of EB, the dichroism amplitude is about half the value at 320 nm. The final extrapolated ($E \rightarrow \infty$) values of ρ at 320, 530, and 265 nm for the ethidium nucleosome complex are given in Table I.

The ethidium dichroism can be explained by clustering of bound dyes. A puzzling feature of the results is the difference in ethidium dichroism measured at 320 and 530 nm. The 530-nm transition of ethidium is thought to be along its short axis and, hence, should be roughly parallel to the DNA base pair short axis in the intercalated structure. Since the DNA 265-nm transition moments are oriented predominantly in this direction, we expected to find similar nucleosome dichroism values at 265 and 530 nm. The substantial difference indicated in Table I is not in agreement with that expectation. This result can be explained if the bound ethidium residues are clustered at positions along the superhelix, with the period of bound clusters determined by the DNA helix repeat. For example, if ethidium intercalation occurs primarily when the DNA minor groove faces away from the nucleosome surface, the bound ethidium residues would have a different average angular orientation than the DNA base transition moments, which are averaged over an entire double-helix repeat.

The rotational orientation time increases substantially on complex formation. We measured the exponential time constant for the field-induced orientation curve with varying amounts of dextran added to the buffer to increase the viscosity. The resulting time constants τ_c were extrapolated to zero added dextran concentration, as described previously (Crothers et al., 1978), yielding the time constants reported in Table I. The rotational orientation of nucleosomes with ethidium bound is slowed by nearly a factor of 4 from the value in the absence of ethidium. Like the change in dichroism, this

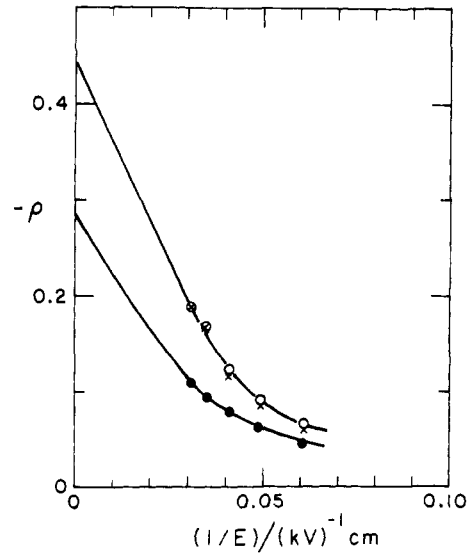

FIGURE 8: Field dependence of reduced dichroism of NC and the NC–EB complex. (●) NC at 265 nm; (× and ○) the NC–EB complex at 320 and 265 nm, respectively. E is the applied electric field in kV cm^{-1}. The solid line is the theoretical field dependence expected if the dipole moment is field independent. Buffer TE/3 (4.3 mM ionic strength), 4 °C; r = 0.06 (EB per DNA base pair).

Table I: Properties of Nucleosomes with and without Ethidium

	ρ_{265} [a]	ρ_{320}	ρ_{530}	τ_c [b] (μs)
free nucleosome	−0.28 ± 0.02			0.8
nucleosome plus ethidium, r = 0.06	−0.45 ± 0.05	−0.45 ± 0.05	−0.25 ± 0.02	3.0
cross-linked nucleosome plus ethidium, r_{added} = 0.06	−0.28 ± 0.02			

[a] ρ_i is the reduced dichroism at wavelength i extrapolated to infinite field. [b] τ_c is the field-induced orientation time, defined by $\rho(t) = \rho(\infty)\exp(-t/\tau_c)$, ignoring fast transients. τ_c was extrapolated to zero-added dextran concentration as described previously (Crothers et al., 1978). T = 4 °C.

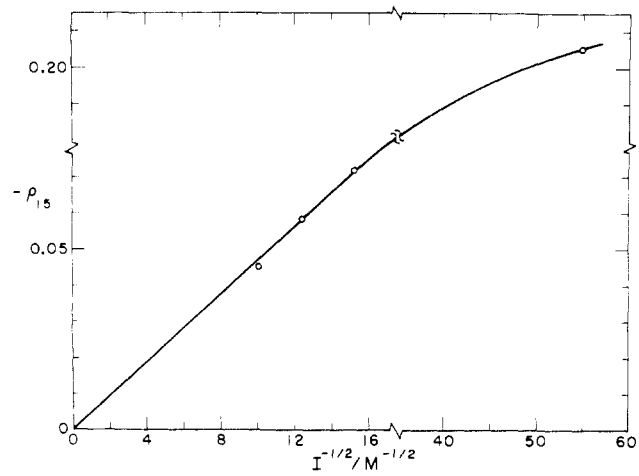

FIGURE 9: Salt concentration dependence of the dichroism of the NC–EB complex, at constant electric field strength, $r = 0.06$ (EB per DNA base pair), $\lambda = 266$ nm, $T = 4$ °C, and ρ_{15} as described in Figure 7. The ionic strength (I) was varied by dilution of TE buffer. The results show a roughly linear variation of the reduced dichroism ρ_{15} with $I^{-1/2}$, a quantity proportional to the Debye radius in the ionic solution.

result also implies a substantial structural alteration of the particle upon drug binding.

Ethidium-bound nucleosomes orient with their superhelical axes parallel to the electric field. In our earlier work we showed that electric field induced orientation mechanisms of particles containing DNA superhelices can be divided into two classes (Hogan et al., 1978; Crothers et al., 1978; Klevan et al., 1978a,b).

Case 1. The orientation axis (parallel to the field direction) is the superhelix axis, with the C_2 symmetry axis perpendicular to the field. This mechanism is found for DNA (Hogan et al., 1978) and the complex between DNA and the histone H3–H4 tetramer (Klevan et al., 1978b) and is characterized by a linear dependence of the apparent dipole moment on the reciprocal square root of the ionic strength ($I^{-1/2}$) (which is proportional to the Debye radius in the solution). In this case the field-induced rotational correlation time τ_c is related to the rotational diffusion time D_r by

$$\tau_c = \frac{1}{6D_r} \quad \text{(superhelix axis orientation)}$$

Case 2. The orientation axis is the C_2 symmetry axis, with the superhelix axis perpendicular to the field. This mechanism is found for nucleosomes in both high and low salt and appears to result when the superhelix length is small compared to its diameter. C_2 axis orientation implies orientation due to a permanent dipole moment, and we have found this process to be characterized by a dipole moment whose magnitude is independent of salt concentration (as long as the particle's shape does not vary with salt concentration). In this case the field-induced rotational correlation time is related to D_r by

$$\tau_c = \frac{1}{2D_r} \quad (C_2 \text{ axis orientation})$$

Figure 9 shows that the apparent dipole moment of ethidium-bound nucleosomes ($r = 0.06$), as estimated from the constant-field dichroism, varies linearly with $I^{-1/2}$ over the salt range in which the nucleosome itself has constant shape and constant dipole moment. Hence, we conclude that nucleosomes in the presence of ethidium orient with the superhelix axis parallel to the field. The switch in orientation mechanism is probably caused by the lengthening of the superhelix axis, which is implied by the sharply increased orientation time.

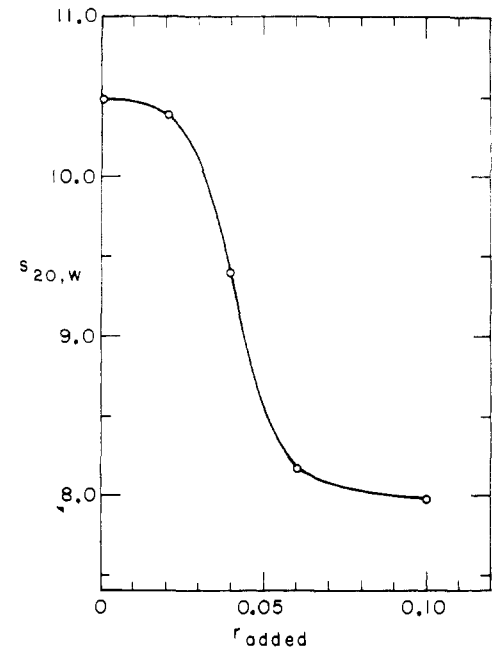

FIGURE 10: Variation of the sedimentation coefficient $s_{20,w}$ of the nucleosome–ethidium complex with ethidium content, r_{added} = ethidium residues added per DNA base pair. TE buffer.

The sedimentation coefficient of nucleosomes decreases on complex formation. Figure 10 shows the variation of the sedimentation coefficient $s_{20,w}$ of the nucleosome–ethidium complex with increasing amounts of added ethidium. As also seen for the dichroism in Figure 7, the change of $s_{20,w}$ is sigmoidal with r. $s_{20,w}$ reaches a plateau value of about 8.2 ± 0.1 S at $r \geq 0.06$.

DMS cross-linked nucleosomes bind ethidium weakly and are not distorted. Figure 5 shows that the affinity of nucleosomes for ethidium is reduced by roughly 2 orders of magnitude when the nucleosomes are cross-linked with DMS, and Table I and Figure 7 indicate that the dichroism of cross-linked nucleosomes is unaltered by the addition of ethidium. Hence, we conclude that the nucleosome distortion implied by the change in ρ and τ_c is required for ethidium binding and must involve protein–protein movements. Cross-linking blocks distortion and consequently prevents binding.

Ethidium binds to nucleosomes weakly in the presence of Mg^{2+}. We found that the addition of Mg^{2+} to the ethidium–nucleosome complex in TE buffer to a final Mg^{2+} concentration of 10 mM causes the intrinsic fluorescence enhancement of ethidium to drop to 20% of that in the absence of Mg^{2+}. Addition of Mg^{2+} to free DNA to the same concentration decreased the fluorescence by a much smaller amount, to 80% of its value without Mg^{2+}. Hence, 10 mM Mg^{2+} causes the binding of EB to nucleosomes to be weaker than the binding to DNA, in contrast to the stronger binding in TE buffer.

The size of DNA fragments produced by DNase II digestion of nucleosomes remains constant as ethidium is added, but the bandwidth increases. The digestion of the EB–NC complex by DNase II is a suitable probe for the structure of the EB–NC complex, because DNase II does not require divalent cations, which may affect the binding of EB with NC. As shown in Figure 11, the individual fragment bands of the DNase II limit digestion pattern of nucleosome-bound DNA became smeared as more than five to six ethidium molecules were bound to each nucleosome. However, the main repeating pattern was maintained. The digestion pattern of DNA in

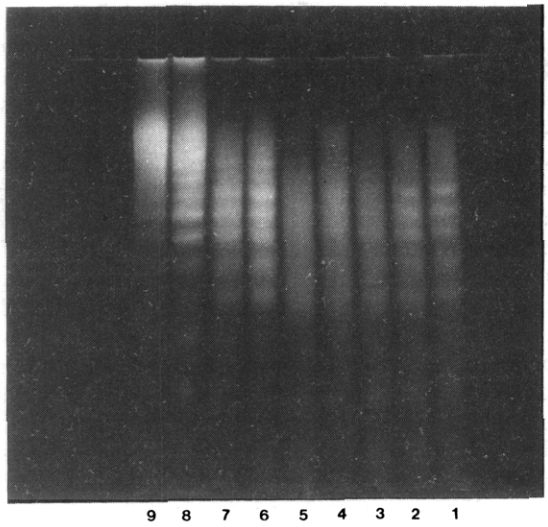

FIGURE 11: Effect of ethidium on the DNase II and DNase I digestion patterns of nucleosomes. From right to left: (1–5) nucleosomes were digested with DNase II in TE buffer, pH 7, at varying amounts of added ethidium: (1) $r = 0$; (2) $r = 0.02$; (3) $r = 0.04$; (4) $r = 0.06$; (5) $r = 0.1$. (6 and 7) DMS-cross-linked nucleosomes were digested with DNase II in TE buffer, pH 7: (6) $r = 0$; (7) $r = 0.1$. (8 and 9) Nucleosomes were digested with DNase I in 10 mM Tris and 10 mM Mg^{2+}, pH 7.5: (8) $r = 0$; (9) $r = 0.1$.

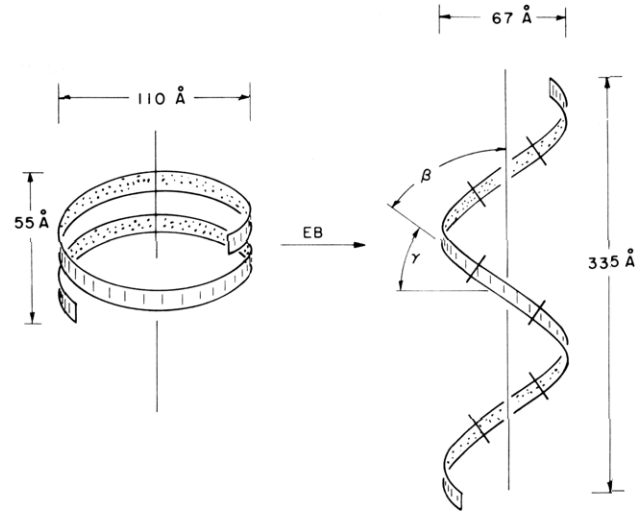

FIGURE 12: Schematic presentation of the proposed model for structure of nucleosome unfolded in presence of ethidium. A superhelix of dimensions 355 × 67 × 67 Å (right) is produced by binding of ethidium ($r \simeq 0.06$) to DNA in nucleosomes (left). The DNA can be viewed as a ribbon whose edge is drawn through successive helix repeats [spaced 10.4 base pairs apart (Wang, 1979)]. Since this repeat distance is retained in the complex, the ribbon must be kept flat against the surface of the cylinder in the elongated NC–EB complex. It is shown in the text that a duplex unwinding of 39° per bound EB is required to produce the model shown.

cross-linked nucleosomes, or the DNase I digestion pattern of native nucleosomes with magnesium present, showed no change on the addition of ethidium to an r value as high as 0.1.

Discussion

Our results show that ethidium binding strongly distorts the structure of 140 base pair nucleosomal core particles (Figures 7, 8, and 10), but it does not preferentially dissociate any histone species from DNA (Figure 1). Binding probably occurs by intercalation into nucleosomal DNA (Figures 2–4) and results in strong immobilization of the drug. In 13 mM ionic strength (TE buffer) binding of ethidium to nucleosomes is stronger than to the same amount of DNA free in solution, as long as r is less than 0.07 (Figure 5). However, cross-linking the nucleosomal proteins virtually abolishes binding, and addition of Mg^{2+} strongly reduces the affinity, compared to the effect on free DNA. Binding makes the DNase II digestion pattern more diffuse but does not systematically shift the band positions (Figure 11). The remainder of our comments serve to describe simple structural and thermodynamic models for the binding process.

Structural Model for the Ethidium–Nucleosome Complex. The binding of 8–10 ethidium residues to a nucleosome increases the negative reduced dichroism from 0.29 to 0.45. This is accompanied by an increase in the rotational orientation time from 0.8 to 3 μs ($T = 4$ °C) and a decrease in the sedimentation coefficient from 10.5 to 8.2 S. These results imply that the nucleosome is converted to a more extended structure, and the salt concentration dependence of the apparent dipole moment indicates that orientation occurs along the elongated superhelix axis. In addition, the model must account for the constancy of the base-pair interval between preferred nuclease digestion sites.

To obtain a specific model, we assume that the nucleosome–ethidium complex can be described as an elongated superhelix. Our results specify the pitch angle (β) and length (L) of the superhelix within reasonably precise limits. Assuming the transition moment angle α in eq 1 is 73° as found for DNA (Hogan et al., 1978) and solving for β from the measured value ρ_∞ (–0.45) yield $\beta = 39°$. Alternatively, the limiting value of $\alpha = 90°$, which we found to be consistent with the data for DNA in nucleosomes (Crothers et al., 1978), yields $\beta = 43°$. Hence, we adopt the intermediate value $\beta = 41°$, which is reasonably close to both of the two limits.

The rotational correlation time $\tau_c = 1/6D_r$ can be related to the length L and radius b of the superhelix by using the equation given by Broersma (1960) for cylinders

$$D_r = \frac{3kT}{\pi\eta_0 L^3}\left[\ln\left(\frac{L}{b}\right) - 1.57 + 7\left[\frac{1}{\ln(L/b)} - 0.28\right]^2\right] \quad (2)$$

in which η_0 is the solvent viscosity. Assuming that b must be between the limits 55 Å (as found for nucleosomes) and 13 Å (as characteristic of free DNA), the corresponding values of L that give $\tau_c = 3.0$ μs ($T = 277$ K; $\eta_0 = 0.0157$ P) are 320 and 430 Å.

The superhelix dimension must also yield plausible values for the DNA contour length $\mathcal{L} = L/\cos\beta$. After correction for lengthening of the DNA by 2.7 Å per bound ethidium (Hogan et al., 1979) ($r = 0.06$; 140 base pairs; $\beta = 41°$), the calculated DNA length per base pair is 3.91 Å when $L = 430$ Å and is 2.86 Å when $L = 320$ Å. The former number is clearly outside the range of plausible values as judged, for example, by electron microscopy (Vollenweider et al., 1978; Griffith, 1978). Taking 3.4 Å to be the maximum allowed rise per base pair, we estimate a maximum value of $L = 377$ Å. Therefore, we conclude that L must lie between about 320 and 380 Å.

A compromise model which fits these limits, shown in Figure 12, is characterized by $L = 335$ Å and diameter $= 2b = 67$ Å. The calculated rise per DNA base pair is 3.0 Å (corrected for ethidium lengthening), and the number of turns about the superhelical axis (calculated from the superhelix radius and pitch angle) is 1.4, the same as the value inferred for nucleosomes from dichroism measurements (Crothers et al., 1978).

The measured sedimentation coefficient of the NC–EB complex is in reasonable agreement with the model shown in

Figure 12. The sedimentation coefficient s is given by

$$s = \frac{M_r \phi_2}{N_A f}$$

in which M_r is the molecular weight, $\phi_2 = (\partial\rho/\partial c)_\mu$ is the density increment at constant chemical potential of dialyzable species, and N_A is Avogadro's number. The fictional coefficient f can be expressed as

$$f = \frac{3\pi\eta_0 L}{\ln (L/2b) + \gamma}$$

Using $M_r = 2.1 \times 10^5$, $\phi_2 = 0.66$ [estimated from the results obtained for nucleosomes by Olins et al. (1976)], and $\gamma = 0.43$ for a particle of axial ratio $L/2b = 5$ [as tabulated by Tirado & Garcia de la Torre (1979)], we obtain $s_{20,w} = 7.7$ S for the proposed model of the nucleosome–ethidium complex shown in Figure 12. The measured value of 8.2 S is slightly higher, but, considering the uncertainty in the density increment of the complex, we consider the agreement satisfactory. Strict adherence to a simultaneous fit of the sedimentation coefficient and rotational correlation time would require a model roughly 10% narrower and 3% longer, adjustments which lie within the uncertainty range of the proposed model.

The model shown in Figure 12 also explains the retention of the spacing between preferred nuclease digestion sites as unwinding occurs. The structure is drawn in the form of a ribbon wound about the surface of a cylinder, analogous to the models given by Crick (1976). Each edge of the ribbon is drawn through the DNA helix repeat element every 10.4 base pairs (Wang, 1979; Lutter, 1979). Consequently, if the ribbon is kept flat against the surface of the cylinder, the repeat interval between equivalent sites as viewed normal to the surface of the cylinder will remain at 10.4 base pairs.

The equations given by Crick (1976) can be used to calculate the untwisting of the double helix required to produce the model in Figure 12. Let ΔLk be the change in the linking number of the two DNA strands relative to their value in free DNA, the latter being represented by the linear ribbon flattened in a plane. The change in linking number per nucleosome for the superhelical structure in Figure 12 is (Crick, 1976)

$$\Delta\text{Lk} = n$$

in which n is the number of turns about the superhelical axis per nucleosome. (Lk is a property of a closed curve, so ΔLk must be obtained as described by Crick (1976) by extending the nucleosomal helix over many repeats, closing the curve with a linker of ΔLk = 0, and dividing the total ΔLk by the number of nucleosomes.) Since the model in Figure 12 has $n = 1.4$ for both the nucleosome and the nucleosome–ethidium complex, the net change in linking number $\delta(\Delta\text{Lk})$ per nucleosome upon ethidium binding is zero. Notice that the equivalent of $\delta(\Delta\text{Lk})$ is also zero when ethidium binds to and reverses the superhelical turns in a closed circular DNA.

Given that $\delta(\Delta\text{Lk})$ is zero for the binding process in Figure 12, the averaged sum of changes in twist δTw and writhe δWr must also be zero when binding occurs:

$$\delta\text{Tw} + \delta\text{Wr} = 0$$

The twist of a ribbon kept flat against the surface of a cylinder in a left-handed superhelix is (Crick, 1976; Fuller, 1978)

$$\text{Tw} = -n \sin\gamma$$

in which $\gamma = 90 - \beta$ describes the superhelix pitch. Taking $\gamma = 5.9°$ from the known dimensions of the nucleosome, we get Tw(nucleosome) = −0.14 turn. Similarly, using $\gamma = 90 - 41° = 49°$ gives −1.06 for Tw(nucleosome–ethidium complex). Hence, δTw = −0.91 turn. Therefore, the unwinding angle per ethidium is $0.91 \times 360°/(140r) = 39°$. This is significantly larger than the value (26°) found for the unwinding of DNA. However, as we show below, the nucleosome is under considerable superhelical stress, and it is plausible that this stress forces a somewhat larger unwinding angle, probably distributed over adjacent base pairs, once the native nucleosomal structure is disrupted. We can also conclude that δWr = 0.91 for the model in Figure 12. Thus, unwinding of the double helix (negative δTw) reduces the left-handed superhelical writhe (positive δWr), just as that found when ethidium relaxes closed circular DNA.

Thermodynamic Model for Binding. In general, curved Scatchard binding isotherms of the kind shown in Figure 5 do not imply a unique model for the complex. The curvature could arise from two (or more) different kinds of binding sites, or it could reflect an anticooperative interaction which causes binding to become weaker as r increases (Bloomfield et al., 1974). Curvature of the binding isotherm of ethidium with free DNA has been explained (Bauer & Vinograd, 1970; Bresloff & Crothers, 1975) by the neighbor exclusion model (Crothers, 1968), according to which each space between base pairs can in principle serve as a binding site, but occupancy of one site excludes binding at the adjacent potential sites on each side.

The two distinguishing features of the nucleosome–ethidium binding isotherm are the very high affinity at low r and the relatively low amount of ethidium bound at saturation. The high initial binding affinity has two possible sources: (a) the binding site could be altered by curvature of the DNA so that the intrinsic affinity is increased; (b) binding could be coupled to release of superhelical stress, thereby increasing the apparent affinity. The second of these two alternatives is consistent with all our observations and closely parallels the interpretation of enhanced ethidium binding to closed circular DNAs. Hence, our thermodynamic model is based on alternative b, but it should be realized that we cannot absolutely eliminate alternative a.

The low saturation value of r for the NC–EB complex probably results from a combination of factors. Neighbor exclusion is expected, as found for free DNA, but in addition the distortion free energy which acts to enhance binding at low r may have the opposite effect at high r. This effect is analogous to the crossover of binding isotherms observed for closed circular and nicked DNAs (Bauer & Vinograd, 1970; Hsieh & Wang, 1975). A further complication is provided by the evidence from both fluorescence depolarization and visible dichroism amplitudes that the bound dyes are more clustered than they would be on free DNA at the same r value. This result can be incorporated into the model by assuming that only a fraction of the potential binding sites on DNA are actually available in nucleosomes, the remainder being blocked by protein–DNA interactions. Bound ethidium residues are assumed to cluster in the available regions.

To accommodate all of these factors, we propose a thermodynamic model for the complex which has the following general features. (1) The free energy of distortion (G_d) of the nucleosomal particle, which includes the free energy of release of DNA superhelical stress and any free energy contributions due to the distortion of nucleosomal proteins which is required for binding, depends parabolically on r

$$G_d = \frac{a_1 RT(r - r_c)^2}{2}$$

in which r_c is the critical value of r at which the distortion

energy is minimized. (2) A fraction f of the DNA base pairs in nucleosomes is available for drug binding. (3) Within the available binding regions, the binding equilibrium is described by the neighbor exclusion model (Crothers, 1968): the intrinsic binding constant to an isolated intercalation site is K, and at least $n^* - 1$ empty intercalation sites must intervene between adjacent bound drug molecules.

The Scatchard binding isotherm for the neighbor exclusion model for free DNA, which can be derived in a number of equivalent ways (McGhee & von Hippel, 1974; Crothers, 1968), is

$$\frac{r}{m} = K(1 - nr)\left[\frac{1 - nr}{1 - (n-1)r}\right]^{n-1} \quad (3)$$

in which m is the free drug concentration and n is found to be 2 for binding of ethidium to free DNA. The analogous expression for binding to nucleosomes is

$$\frac{r}{m} = fK(1 - n^*r/f)\left[\frac{1 - n^*r/f}{1 - (n^* - 1)r/f}\right]^{n^*-1} \exp[-a_1(r - r_c)] \quad (4)$$

In this expression the measured values of r are divided by f to correct them to the acutal values r/f in the available binding regions. The term $\exp[-a_1(r - r_c)]$ corrects for the distortion energy, as has been shown in several earlier papers on closed circular DNA (Bauer & Vinograd, 1970; Hsieh & Wang, 1975).

The parameter in eq 4 which is most uncertain is f, which we presently have no direct way to measure. The energy transfer and dichroism data suggest values between 0.4 and 0.8. Numbers in the upper end of this range give better agreement with the experimental binding isotherm. Once f is assumed, a_1 and r_c can be estimated by a method analogous to the approach of Hsieh and Wang (see Appendix). The theoretical curve illustrated in Figure 5 was calculated with $K = 4.7 \times 10^5$ M^{-1} (determined from the binding isotherm for free DNA), $f = 0.7$, $n^* = 2$ (assumed to be the same as for free DNA), $r_c = 0.11$, and $a_1 = 14$. The value of a_1 is close to the result found by Hsieh & Wang (1975) for the distortion free energy of closed circular DNA. The critical value of r, $r_c = 0.11$, does not correspond to the point at which the two isotherms cross in Figure 5 because of the factor f. The calculated curve in Figure 5 agrees with experiment within the scatter of the data.

In summary, the thermodynamic model for binding states that the affinity is enhanced by the release of distortion energy which accompanies binding. The presumed structural reason for this enhancement is that local untwisting of the DNA duplex is needed in order to allow formation of the elongated DNA superhelix shown in Figure 12. The requirement for untwisting must reflect the protein–DNA interactions in the elongated complex. If, as the DNase II digestion data imply, a 10.4 base pair repeat (as viewed from the surface of the superhelix) is maintained in the elongated complex, then untwisting *must* accompany elongation. Hence, the particle cannot open spontaneously in absence of ethidium, because this would require an unacceptable local untwisting of the DNA duplex.

The estimated angle of untwisting per bound ethidium, 39°, is somewhat larger than the standard value of 26°. It is plausible that the torsional elasticity of the DNA duplex allows some additional unwinding beyond the 26° which should occur at the intercalation site. This extra unwinding presumably would be spread out over the adjacent base pairs and would occur to an extent determined by simultaneous minimization of the superhelical distortion free energy and the DNA duplex torsional free energy.

A Possible Further Complication. Under our solution conditions we were unable to characterize the binding equilibrium for $r < 0.04$. Both the dichroism and sedimentation results indicate a lag as ethidium is added before detectable structural changes occur. Hence, it is possible that there is an initial cooperative phase of binding, characterized by a barrier to initiating the drug-induced distortion of the nucleosomal particle. Special protein–protein interactions which stabilize the native nucleosome could be responsible for such a barrier. Further work will be required to elucidate the initial stages of drug binding.

Appendix

Evaluation of the Distortion Free Energy of Nucleosomes. The force constant a_1 and the critical value of r (r_c) in the expression for the distortion free energy $G_d = a_1RT(r - r_c)^2/2$ can be evaluated by a procedure closely analogous to that used by Hsieh & Wang (1975), except that we take account of neighbor exclusion in the binding isotherm. At equilibrium the free energy change per base pair $dG = 0$ due to binding ethidium to free DNA can be expressed as

$$dG = (\mu_C - \mu_S - \mu_E)dr \quad (A1)$$

in which μ is the chemical potential, C, S, and E refer to the complex, binding site, and ethidium, respectively. Replacing μ by $\mu = \mu^\circ + RT \ln C$ (assuming a dilute solution) and rearranging give for free DNA

$$dG = \left(\mu^\circ_C - \mu^\circ_S - \mu^\circ_E + RT \ln \frac{P_C}{P_X} - RT \ln C_E\right)dr \quad (A2)$$

in which P_C and P_S are, respectively, the fraction of DNA sites which are present as complex and unoccupied sites. The neighbor exclusion theory for the binding equilibrium provides the relationship (McGhee & von Hippel, 1974)

$$\frac{P_C}{P_S} = \frac{r}{(1 - nr)}\left[\frac{1 - (n-1)r}{1 - nr}\right]^{n-1} \quad (A3)$$

Substituting this result into eq A2 and replacing the first three terms on the right side of eq A2 by $\Delta\mu^\circ$ yield

$$dG = \left[\Delta\mu^\circ + RT \ln \left[\left(\frac{r}{1 - nr}\right) \times \left[\frac{1 - (n-1)r}{1 - nr}\right]^{n-1}\right] - RT \ln C_E\right]dr \quad (A4)$$

The expression for dG for the nucleosome is exactly analogous, except that r/f replaces r, n^* replaces n, and there is an additional additive term dG_d for the distortion free energy:

$$dG^* = dG_d + \left[\Delta\mu^{\circ *} + RT \ln \left[\left(\frac{r/f}{1 - n^*r/f}\right)\left[\frac{1 - (n^* - 1)r/f}{1 - n^*r/f}\right]^{n^*-1}\right] - RT \ln C_E^*\right]dr \quad (A5)$$

At this point we assume that the intrinsic binding affinity is the same for free DNA and nucleosomes, so that $\Delta\mu^\circ = \Delta\mu^*$. Then, using the fact that $dG = dG^* = 0$, we can combine eq A4 and A5 to obtain

$$dG_d = RT\left[\ln\frac{C_E^*}{C_E} + \ln f + (n-1)\ln\frac{1-(n-1)r}{1-nr} + \ln\frac{1-n^*r/f}{1-nr} - (n^*-1)\ln\frac{1-(n^*-1)r/f}{1-n^*r/f}\right]dr \quad \text{(A6)}$$

In this equation, C_E^*/C_E is the ratio of the free ethidium concentration in equilibrium with nucleosomes to the free concentration in equilibrium with DNA, both at the same value of r.

Since G_d depends quadratically on $r - r_c$, we can set

$$dG_d = a_1 RT(r - r_c)dr$$

Therefore

$$a_1(r - r_c) = \ln\frac{C_E^*}{C_E} + \ln f + (n-1)\ln\frac{1-(n-1)r}{1-nr} + \ln\frac{1-n^*r/f}{1-nr} - (n^*-1)\ln\frac{1-(n^*-1)r/f}{1-n^*r/f} \quad \text{(A7)}$$

Equation A7 is used to evaluate a_1 by plotting the right side against r. (Values of f, n, and n^* must be assumed.) The slope is a_1, and $r = r_c$ when the right side of the equation is zero. We found from the data in Figure 5 that $a_1 = 14 \pm 3$ and $r_c = 0.11$, when $n = 2$, $n^* = 2$, and $f = 0.7$.

The total distortion free energy of the nucleosome ΔG_N can be calculated from

$$\Delta G_N = \frac{N a_1 RT r_c^2}{2} \quad \text{(A8)}$$

in which N is the number of base pairs per nucleosome. Substituting the observed values gives $\Delta G_N = 7$ kcal/mol of nucleosome. According to this result, the distortion free energy change due to unwinding the nucleosome by ethidium binding is −7 kcal/mol, when unwinding proceeds to the relaxed state in which $r = r_c$. The negative sign implies that the distortion free energy favors unwinding and, hence, that the nucleosome is under unwinding stress. However, unfolding of the nucleosome is not spontaneous in the absence of ethidium because duplex DNA cannot be sufficiently underwound to produce nucleosome extension. An essential feature of the phenomenon appears to be the requirement for a regular 10.4 base pair spacing per duplex turn even in the extended form of the nucleosome. It is this requirement which demands unwinding in order to produce extension.

References

Angerer, L. M., & Moudrianakis, E. N. (1972) *J. Mol. Biol. 63*, 505–521.

Angerer, L. M., Georghiou, S., & Moudrianakis, E. N. (1974) *Biochemistry 13*, 1075–1082.

Barkley, M. D., & Zimm, B. H. (1979) *J. Chem. Phys. 70*, 2991–3007.

Bauer, W., & Vinograd, J. (1970) *J. Mol. Biol. 47*, 419–435.

Bloomfield, V. A., Crothers, D. M., & Tinoco, I., Jr. (1974) *Physical Chemistry of Nucleic Acids*, pp 410–411, Harper and Row, New York.

Bontemps, J., & Fredericq, E. (1974) *Biophys. Chem. 2*, 1–22.

Bresloff, J. L., & Crothers, D. M. (1975) *J. Mol. Biol. 95*, 103–123.

Broersma, S. (1960) *J. Chem. Phys. 32*, 1626–1631.

Crick, F. H. C. (1976) *Proc. Natl. Acad. Sci. U.S.A. 73*, 2639–2643.

Crothers, D. M. (1968) *Biopolymers 6*, 575–584.

Crothers, D. M., Dattagupta, N., Hogan, M., Klevan, L., & Lee, K. S. (1978) *Biochemistry 17*, 4525–4533.

Foe, V. E., Wilkinson, L. E., & Laird, C. D. (1976) *Cell 9*, 131–146.

Fuller, W. B. (1978) *Proc. Natl. Acad. Sci. U.S.A. 75*, 3557–3561.

Garel, A., & Axel, R. (1976) *Proc. Natl. Acad. Sci. U.S.A. 73*, 3966–3970.

Gottesfield, J. M., Murphy, R. F., & Bonner, J. (1975) *Proc. Natl. Acad. Sci. U.S.A. 72*, 4404–4408.

Griffith, J. D. (1978) *Science 201*, 525–527.

Hogan, M., Dattagupta, N., & Crothers, D. M. (1978) *Proc. Natl. Acad. Sci. U.S.A. 75*, 195–199.

Hogan, M., Dattagupta, N., & Crothers, D. M. (1979) *Biochemistry 18*, 280–288.

Houssier, C., Hardy, B., & Fredericq, E. (1974) *Biopolymers 13*, 1141–1160.

Hsieh, K., & Wang, J. C. (1975) *Biochemistry 14*, 527–535.

Hudson, B., & Jacobs, B. (1975) *Biopolymers 14*, 1309–1312.

Klevan, L., Hogan, M., Dattagupta, N., & Crothers, D. M. (1978a) *Cold Spring Harbor Symp. Quant. Biol. 42*, 207–214.

Klevan, L., Dattagupta, N., Hogan, M., & Crothers, D. M. (1978b) *Biochemistry 17*, 4533–4540.

Lacy, E., & Axel, R. (1975) *Proc. Natl. Acad. Sci. U.S.A. 72*, 3978–3982.

Lapeyre, J. N., & Bekhor, I. (1974) *J. Mol. Biol. 89*, 137–162.

Lawrence, J., Chan, D. C. F., & Piette, L. H. (1976) *Nucleic Acids Res. 11*, 2879–2893.

Lepecq, J. B., & Paoletti, C. (1967) *J. Mol. Biol. 27*, 87–106.

Lutter, L. (1979) *Nucleic Acids Res. 6*, 41–56.

McGhee, J. D., & von Hippel, P. H. (1974) *J. Mol. Biol. 85*, 469–489.

Olins, A. L., Carlson, R. D., Wright, E. B., & Olins, D. E. (1976) *Nucleic Acids Res. 3*, 3271–3291.

Paoletti, J., & Lepecq, J. B. (1971) *J. Mol. Biol. 59*, 43–62.

Paoletti, J., Magee, B. B., & Magee, P. T. (1977) *Biochemistry 16*, 351–357.

Richards, B. M., Pardon, J. F., Lilley, D. M. J., Wooley, J. C., & Worcester, D. L. (1977) *Cell Biol. Int. Rep. 1*, 107–116.

Rill, R. L. (1972) *Biopolymers 11*, 1929–1941.

Scatchard, G. (1949) *Ann. N.Y. Acad. Sci. 51*, 660–672.

Seale, R. L. (1978) *Proc. Natl. Acad. Sci. U.S.A. 75*, 2717–2721.

Tirado, M. M., & Garcia de la Torre, J. (1979) *J. Chem. Phys. 71*, 2581–2587.

Vollenweider, H. J., James, A., & Szybalski, W. (1978) *Proc. Natl. Acad. Sci. U.S.A. 75*, 710–714.

Wang, J. C. (1974) *J. Mol. Biol. 89*, 783–801.

Wang, J. C. (1979) *Proc. Natl. Acad. Sci. U.S.A. 76*, 200–203.

Weintraub, H., & Groudine, M. (1976) *Science 193*, 848–856.

Wu, H. M., Dattagupta, N., Hogan, M., & Crothers, D. M. (1979) *Biochemistry 18*, 3960–3965.